Astrophysical Masers and their Environments
Proceedings IAU Symposium No. 242, 2007
J.M. Chapman & W.A. Baan, eds.

doi:10.1017/S1743921307013592

A compact starburst ring traced by clumpy OH megamaser emission

Rodrigo Parra[1], **John E. Conway**[1],
Moshe Elitzur[2] and **Ylva M. Pihlström**[3]

[1]Onsala Space Observatory, S 43992, Onsala, Sweden
[2]Department of Physics and Astronomy, University of Kentucky, Lexington, KY 40506, USA
[3]Department of Physics and Astronomy, UNM, 800 Yale Blvd NE, Albuquerque, NM 87131, USA

Abstract. We model the OH megamaser emission from the luminous infrared galaxy IIIZw35 as arising from a narrow rotating starburst ring of radius 22 pc enclosing a mass of 7×10^6 $M_\odot$. We show how both the compact and apparently diffuse maser emission from this ring can arise from a single phase of unsaturated maser clouds amplifying background radio continuum. The masering clouds are estimated to have a diameter of <0.7 pc and internal velocity dispersion of $\sim$20 km s^{-1}. We find that the clouds are neither self-gravitating nor pressure confined, and they could be magnetically confined or freely expanding. Their dispersal lifetimes may set the vertical thickness of the ring. For an estimated internal density of 3×10^3 cm^{-3}, cloud masses are of order 24 $M_\odot$. The observed spectral features and velocity gradients indicate that the clouds must be outflowing and escaping the nucleus. The cloud mass outflow rate is estimated to be 0.8 $M_\odot$ yr^{-1}, while the star formation rate is $\sim$19 $M_\odot$ yr^{-1}. Associated ionised gas, possibly generated from dissipated clouds, provides free-free absorption along the source axis, explaining the observed East-West asymmetries. We show that the clumpiness of a maser medium can have a dramatic effect on what is observed even in a relatively low gain OH megamaser. Specifically, in IIIZw35 our clumpy maser model naturally explains the large line to continuum ratios, the large 1667MHz:1665MHz line ratios and the wide velocity dispersions seen in the compact maser spots. Other astrophysical masers showing both compact and apparently diffuse emission might be explained by similar clumpy structures.

1. Introduction

Extra-galactic OH megamaser (OH MM) emission is generally associated with compact (<100 parsec) starburst activity in the centres of IR luminous galaxies. Observations of this maser emission provide a unique method of studying the structure and kinematics of galactic nuclei at parsec (pc) resolution without dust obscuration effects. Measurements of velocity gradients and line widths (e.g. Pihlström *et al.* 2001) already provide important constraints on stellar mass densities and turbulent velocities in IR luminous galaxies. Potentially OH MM can also tell us about the size, density and temperature of molecular clouds in the central ISM of starburst galaxies. However, to accomplish these goals a better understanding of the OH MM phenomenon is required.

In the standard model (see Baan 1989; Lonsdale 2002), OH MM emission is generated by low gain ($|\tau| \lesssim 2$) unsaturated amplification of background continuum by a foreground OH amplifying medium. Although this medium is comprised of discrete OH clouds it is implicitly assumed that there are many such clouds and they individually have very low gains. These clouds therefore form an effective *gas* in which statistical fluctuations in cloud number between different lines of sight are unimportant and so the maser opacity varies slowly across the source. Given these assumptions the amplifying medium is often described as a *diffuse screen*.

Consistent with the standard model, early VLA and MERLIN observations showed that OH maser and continuum emission overlapped. However, VLBI observations of Arp 220 resulted in the detection of both compact continuum (Diamond *et al.* 1999; Smith *et al.* 1998) and compact OH maser emission (Lonsdale *et al.* 1994, 1998). Remarkably, these bright maser spots were not spatially coincident with the continuum spots, and some displayed extreme line-to-continuum ratios (LCR) in excess of 800 (Lonsdale *et al.* 1998). These observations were clearly inconsistent with diffuse screen models. Slightly less extreme compact maser emission was subsequently detected in other sources (Trotter *et al.* 1997; Diamond *et al.* 1999; Klöckner *et al.* 2003; Klöckner & Baan 2004). These same sources also contain diffuse maser components which account for between 50% and 90% of the total maser flux density. It has been suggested that the compact masers occur in saturated, perhaps collisionally pumped regions, while the diffuse component comes from an extended unsaturated, radiatively pumped screen fully consistent with the standard model (Lonsdale *et al.* 1998; Diamond *et al.* 1999).

One of the clearest cases of an OH MM showing both compact and diffuse maser emission is the LIRG IIIZw35. Two groups of compact masers were detected in VLBI observations (Trotter *et al.* 1997; Diamond *et al.* 1999) recovering ∼50% of the total OH maser emission seen on MERLIN scales (Montgomery & Cohen 1992). Most of the missing OH maser flux was found to be in a rotating OH maser ring using EVN+MERLIN observations (Pihlström *et al.* 2001). The previously known compact masers lie at the tangents of this ring. P01 explained both diffuse and compact masers using a mechanism based on a single phase of small OH masering clouds (∼1 pc) amplifying background continuum. At the ring tangents multiple overlaps between clouds in space and velocity are likely due to the increased path length through the ring. These multiple cloud overlaps give rise to the bright compact maser features. Elsewhere, at the front and back of the ring where there are few such cloud overlaps, the emission consists of many weak maser spots. These spots are too weak to be detected individually in high resolution observations but in low resolution observations they are averaged together and give rise to an apparently diffuse emission.

In Parra *et al.* (2005) we investigate in greater depth the *clumpy ring model* proposed in Pihlström *et al.* (2001). We fully consider the spectral and kinematical properties of the maser clouds. We also model the continuum emission in a geometrically and physically consistent manner. Using numerical simulations we demonstrate that most of the available OH maser observations of IIIZw35 can be explained using an improved version of the Pihlström *et al.* (2001) model. Most of the input parameters for these simulations are constrained directly by the observations. Our modelling also illuminates general properties of maser ring geometries and clumpy maser media.

2. Description of the Model

The IIIZw35 OH MM observations are fitted by an inclined axisymmetric model in which both OH clouds and continuum emission coexist within circumnuclear rings (see Figure 1). In order to reconcile such a symmetric geometry with the observed East-West asymmetry in both line and continuum emission, our model also includes a bi-cone of free-free absorption which covers the eastern side of the source. This obscuration defines the maser ring orientation requiring the eastern side to be the most distant. Note that the existence of a free-free absorbing component is supported by independent evidence (Chapman *et al.* 1990). Physically the free-free absorbing cone could be the base of an outflowing superwind such as is often observed in energetic starbursts (Heckman 2003).

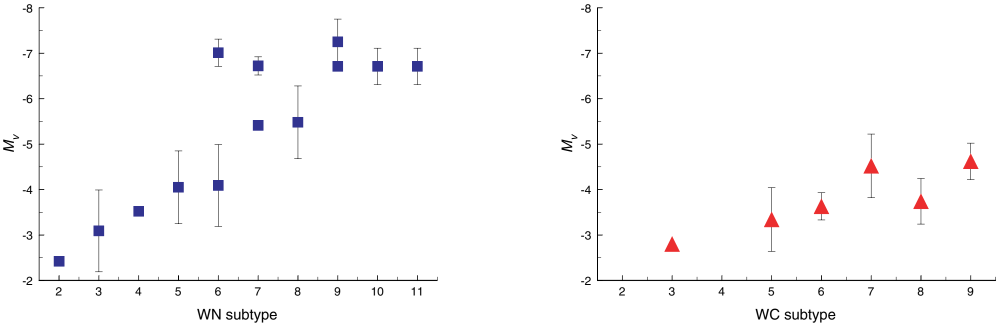

Figure 1. Cross section of the starburst ring plus outflow model proposed for IIIZw35. The proposed ring has internal radius of 22 pc, radial thickness of 3 pc and height of 6 pc. The rotation velocity is 57 $\mathrm{km\,s^{-1}}$ with the northern side being redshifted. The volume defined by the ring is filled with independently orbiting molecular clouds of diameter 0.7 pc, internal velocity dispersion of 20 $\mathrm{km\,s^{-1}}$ and mean density of $3{\times}10^3 \leqslant N_{\mathrm{H}_2} < 10^5$ $\mathrm{cm^{-3}}$. These clouds are assumed to be the source of the OH maser emission. The mechanical energy released by supernova explosions occurring in the equatorial plane of the ring at a rate of $\nu_{\mathrm{SN}} \sim 0.9$ $\mathrm{year^{-1}}$, pushes away from the ring plane the molecular clouds. These clouds are not confined but are instead freely expanding and outflowing away from the ring to eventually dissipate and form a cone of obscuring ionised gas. Although the OH molecules are expected to be in a more extended region than the ring, as suggested by the OH absorption features observed by Pihlström *et al.* (2001), the necessary conditions for maser action (e.g. pumping) are fulfilled only within the ring (see Parra *et al.* 2005).

Although the total maser emission is weaker on the eastern side, the LCR is about factor of 2 larger there than on the western side. This difference is explained if more of the seed continuum emission is background to the OH ring on the east side. This naturally occurs if *most* of the bright continuum emission comes from a larger radius than the OH masering gas. This is corroborated by the fact that the observed continuum radio source is larger than the megamaser source. The proposed geometry also predicts that the brightest masers do not occur exactly at the maser ring tangents but slightly to the east of the tangent points, just as found by the observations of Trotter *et al.* (1997) and Diamond *et al.* (1999).

The properties of the different components of the model are estimated in a detailed way from observations in Parra *et al.* (2005). These parameters are subsequently used in Monte-Carlo simulations to produce the results shown in Figure 2.

3. Conclusions

Observations of distinct regions of compact and apparently diffuse maser emission in OH MM have been used by other authors to argue for two distinct physical phases of OH masers (see Lonsdale *et al.* 1998; Diamond *et al.* 1999). In contrast, the mechanism discussed in Parra *et al.* (2005) explains both types of maser structures using a single phase of low opacity clouds within a thin circumnuclear ring.

The fact that the maser amplifying medium is composed of clouds is found *essential* to explain the range of maser brightness around the ring at low resolution. The same clouds also explain the bright maser spots seen only at the ring tangents in terms of multiple cloud overlaps in both space and velocity. The brightest features in our model arise from the alignment of 5 clouds giving a total maser optical depth of 7.5, well below the threshold of ~13 required for saturation (Elitzur 1992). It is also important to remember that saturation depends on the angle averaged intensity implying that very large maser

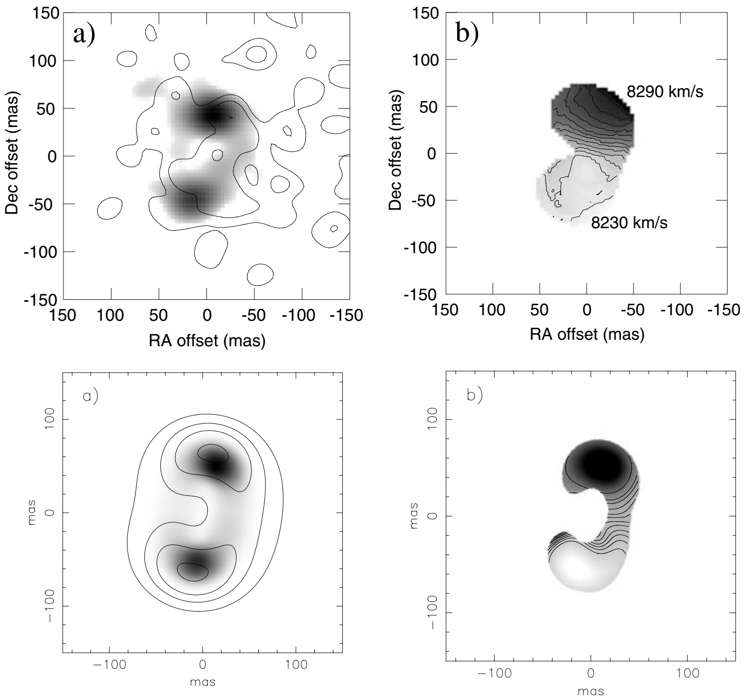

Figure 2. Comparison between observations and numerical simulations. The top row shows images reproduced from P01 showing observations of OH maser and continuum emission at EVN+MERLIN resolution **Top-Left** Greyscale shows the velocity integrated OH emission at a resolution of 34×29 mas. The contours show continuum emission at the same resolution. Contour levels are at -1,1,2, and 4 times the 3σ noise of 0.42mJy/beam. **Top-Right** Corresponding OH maser velocity centroid field. The greyscale is between 8224 (lightest grey) and 8300 $\mathrm{km\,s^{-1}}$ (black). Contours are from 8230 $\mathrm{km\,s^{-1}}$ increasing at 5 $\mathrm{km\,s^{-1}}$ intervals up to 8290 $\mathrm{km\,s^{-1}}$. **Bottom-Left and Right** Same as top row but synthesized from a single realisation of our model (see Parra *et al.* 2005)

brightness temperatures can be achieved whenever the maser beaming angle is small. Such small angles arise naturally in our overlapping cloud model (see Parra *et al.* 2005).

The proposed model can explain the spectra of both the compact spots and the apparently diffuse areas of emission. The fact that the OH clouds are outflowing from the ring midplane explains the large velocity gradients observed amongst the compact maser spots. The model is also able to reproduce the LCRs in the bright spots and diffuse regions, and the large value of the 1667MHz:1665MHz line ratio in the compact spots.

We find that the OH masering ring is relatively narrow in radius which could be explained either in terms of a narrow circumnuclear ring of star formation, or due to the strong sensitivity of maser pumping to physical conditions which vary gradually with radius. The ring we find is narrower but qualitatively similar to those that have been produced in numerical simulations (Wada & Norman 2002; Wada & Tomisaka 2005).

Finally, the model seems to successfully apply to other sources like IRAS 17208–0014 (Momjian *et al.* 2006) or the eastern nucleus of Arp 220.

Acknowledgements

R. P. thanks the University of Kentucky for a most delightful month, which helped in bringing this paper forward to submission. J.C gratefully acknowledges support from the Swedish science research council (VR). M.E. gratefully acknowledges the partial support of NSF.

References

Baan, W. 1989, ApJ, 338, 804
Chapman, J., Staveley-Smith, L., Axon, D., *et al.* 1990, MNRAS, 244, 281
Diamond, P., Lonsdale, C., Lonsdale, C., & Smith, H. 1999, ApJ, 511, 178
Elitzur, M. 1992, Astronomical masers, Vol. 170 (Kluwer Academic Publishers ASSL), 365
Heckman, T. 2003, in Revista Mexicana de Astronomia y Astrofisica Conference Series, 47–55
Klöckner, H.-R. & Baan, W. 2004, A&A, 419, 887
Klöckner, H.-R., Baan, W., & Garrett, M. 2003, Nature, 421, 821
Lonsdale, C. 2002, in IAU Symposium, 413
Lonsdale, C., Diamond, P., & Smith, H. 1994, Nature, 370, 117
Lonsdale, C., Lonsdale, C., Diamond, P., & Smith, H. 1998, ApJ, 493, L13
Momjian, E., Romney, J., Carilli, C., & Troland, T. 2006, ApJ, 653, 1172
Montgomery, A. & Cohen, R. 1992, MNRAS, 254, 23P
Parra, R., Conway, J., Elitzur, M., & Pihlström, Y. 2005, A&A, 443, 383
Pihlström, Y., Conway, J., Booth, R., Diamond, P., & Polatidis, A. 2001, A&A, 377, 413
Smith, H., Lonsdale, C., Lonsdale, C., & Diamond, P. 1998, ApJ, 493, L17
Trotter, A., Moran, J., Greenhill, L., Zheng, X., & Gwinn, C. 1997, ApJ, 485, L79
Wada, K. & Norman, C. 2002, ApJ, 566, L21
Wada, K. & Tomisaka, K. 2005, ApJ, 619, 93